J. Chem. Sci. Vol. 124, No. 4, July 2012, pp. 801–807.

Kinetic studies on substitution of *cis*-diaqua-chloro-tris-(dimethyl sulphoxide)-ruthenium(II) complex with some dipeptides in aqueous medium

ARUP MANDAL, PARNAJYOTI KARMAKAR, SUBHASIS MALLICK, BIPLAB K BERA, SUBALA MONDAL, SUMON RAY and ALAK K GHOSH*

Department of Chemistry, The University of Burdwan, Burdwan 713 104, India
e-mail: alakghosh2002@yahoo.co.in

MS received 29 November 2011; revised 21 January 2012; accepted 7 February 2012

Abstract. The kinetics of interaction between *cis*-$[RuCl(Me_2SO)_3(H_2O)_2]^+$ and some selected dipeptides such as glycyl glycine(gly gly), glycyl alanine(Gly-L-ala) and glycyl-L-leucine(gly leu) has been studied spectrophotometrically as a function of $[RuCl(Me_2SO)_3(H_2O)_2^+]$, [dipeptide] and temperature at a particular pH(5.0), where the substrate complex exists predominantly as a diaqua species (in aqueous solution) and dipeptides as the zwitter ions. The reaction has been found to proceed via two distinct consecutive steps i.e., it shows a non-linear dependence on the concentration of dipeptide: first process is dependent and the second step is independent of ligand concentration respectively. The rate constants for the processes are: $k_1 \sim 10^{-3}s^{-1}$ and $k_2 \sim 10^{-5}s^{-1}$. The activation parameters were calculated from Eyring plots suggests an associative mechanism for the interaction process. From the temperature dependence of the outer sphere association equilibrium constants, the thermodynamic parameters were also calculated, which gives a negative ΔG^0 value at all temperatures studied, supporting the spontaneous formation of an outer sphere association complex.

Keywords. Ligand substitution; dipeptides; *cis*-$[RuCl(Me_2SO)_3(H_2O)_2]^+$; kinetics.

1. Introduction

Carcinostatic properties of platinum complexes, especially of *cis*-platin,[1] involve special impetus to research on interaction of the metal ion with nucleic acid constituents.[2–4] Ruthenium, rhodium, iridium and palladium complexes have also been reported to have considerable antibacterial behaviour.[5,6] Of them, ruthenium complexes seem to be less toxic than *cis*-platin.[7,8] Different studies reveal that a number of ruthenium compounds serve as bacterial mutagens and are capable of damaging genetic material.[9–13] The *in vivo* generation of mixed aqua-ammineruthenium(II) from the ruthenium(III) prodrug should be favoured in a relatively reducing and hypoxic environment provided by the interior of many tumours. Antitumour,[14–17] antiherpes,[18] anti-HIV,[19] antiamebic,[20] anticancer,[21–25] antileukemic[26] and antifungal activity[27,28] are observed in a series of ruthenium complexes.

In continuation of our earlier studies,[29] we report here the interaction of some dipeptides with a different set of donor atoms.

2. Experimental

The reactant *cis*-$[Ru(Me_2SO)_4Cl_2]$ was prepared and characterized according to the method reported by Evans *et al.*[30] The substrate complex $[RuCl(Me_2SO)_3(H_2O)_2]^+$ (**1**) was prepared *in situ* by dissolving the above reactant complex in the aqueous solution (scheme 1).[31]

Cis-$[Ru(Me_2SO)_4Cl_2]$ once dissolved in water, immediately releases the O-bonded dimethyl sulfphoxide molecule.[32]

The products (**2**) of the reaction between the substrate complex and diglycine was prepared by mixing different molar ratios of reactants, *viz.*, 1:1, 1:2 and 1:3 at pH 5.0 and thermostating the mixture at 50°C for 72 h. The absorption spectra of the resultant solutions were recorded using an aqueous ligand solution of appropriate molarity in the reference cell, and it was found that the maximum spectral difference between the product complex and the substrate complex, $[RuCl(Me_2SO)_3(H_2O)_2]^+$ (**1**) was observed at 257 nm (figure 1). The product composition was checked by Job's method of continuous variation as shown in figure 2 and was found to have a 1:1 metal:ligand ratio in the product. The pH was adjusted

*For correspondence

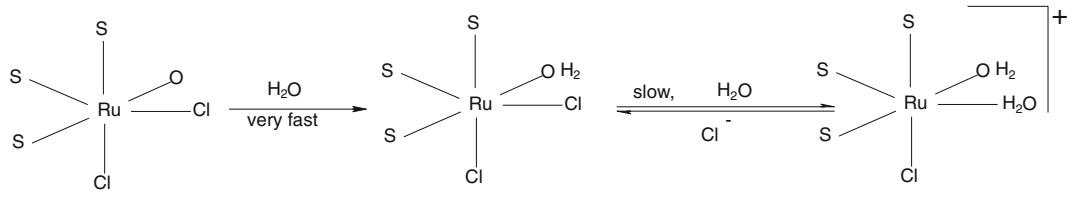

Scheme 1. Chemical behaviour of *cis*-[Ru(Me$_2$SO)$_4$Cl$_2$] in aqueous medium.

by adding a very small amount of dilute *p*-toluene sulphonic acid and NaOH solution such that the concentration of the reaction mixture remains constant. Measurement of pH were carried out with the help of a Sartorius digital pH meter (model PB-11) with an accuracy of ±0.01 units. Doubly distilled water was used to prepare all the solutions. All chemicals used were of AR grade.

Complex (**1**) and diglycine were mixed in 1:1 molar ratio at pH 5.0 and a yellowish product was obtained. The IR spectra of the yellowish product in the KBr disc show strong band at 3435 cm^{-1} together with medium bands at 1630 and 626 cm^{-1}. The strong band at 3435 cm^{-1} indicates that product is hydrated. The asymmetric COO$^-$ stretching frequency of the dipeptides occurs at 1580–1660 cm^{-1} when the group is coordinated to metals, whereas a non-coordinated COO$^-$ group has the γ_{sym} (COO$^-$) stretching at lower frequency. The band at 1630 cm^{-1} is therefore assigned to the γ_{asym} (COO$^-$) of the metal-bounded carboxyl group. An intense band of the amide (>C=O) in the non-coordinated diglycine undergoes a bathochromic ~35 cm^{-1} shift in the IR spectra upon complexation. This is probably due to the involvement of the peptide nitrogen (because of the deprotonation that has taken place) in bonding with Ru(II), which lowers the bond order of the (>C=O) amide group due to resonance stabilization.[33] The 626 cm^{-1} is due to the formation of Ru-N bond in the product.[34]

Conductance measurement also helps us to assign the product formation. With the progress of the reaction there is release of –H$^+$ ion (figure 9) and it is expected that the conductance of the reacting solution increases with the progress of the reaction and this is observed experimentally. Due to the release of –H$^+$ ion, the pH of the resulting solution is found to decrease.

3. Kinetic studies

Kinetic measurements and calculations were carried out in a similar way as reported in an earlier paper.[29] The $k_{1(obs)}$ and $k_{2(obs)}$ values were calculated graphically using the method of Weyh and Hamm.[35]

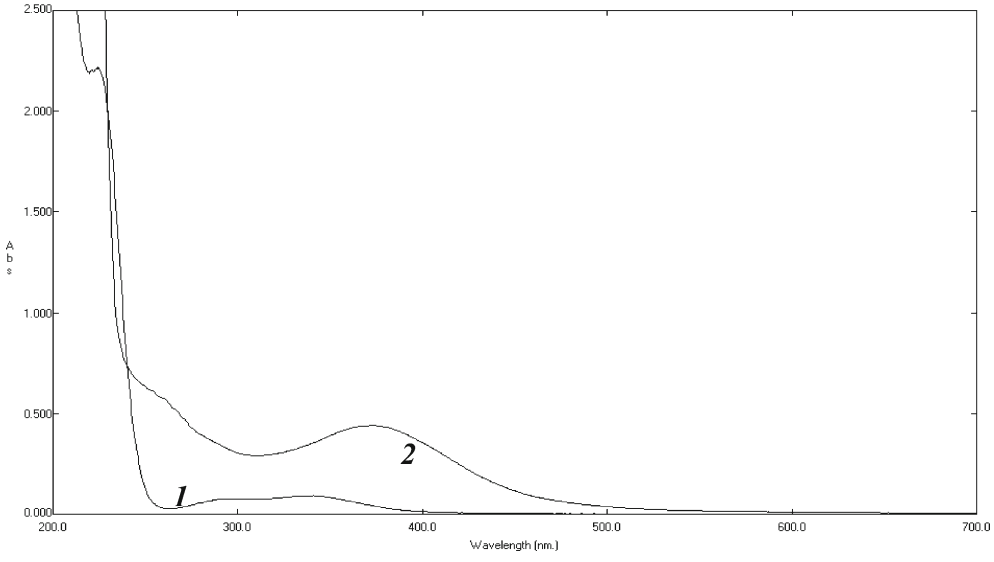

Figure 1. Spectral difference between substrate complex and product. (**1**) [RuCl(Me$_2$SO)$_3$(H$_2$O)$_2^+$] = 1.0 × 10^{-4} mol dm^{-3}; (**2**) [RuCl(Me$_2$SO)$_3$(H$_2$O)$_2^+$] = 1.0 × 10^{-4} mol dm^{-3}, [gly gly] = 2.0 × 10^{-3} mol dm^{-3}, pH = 5.0.

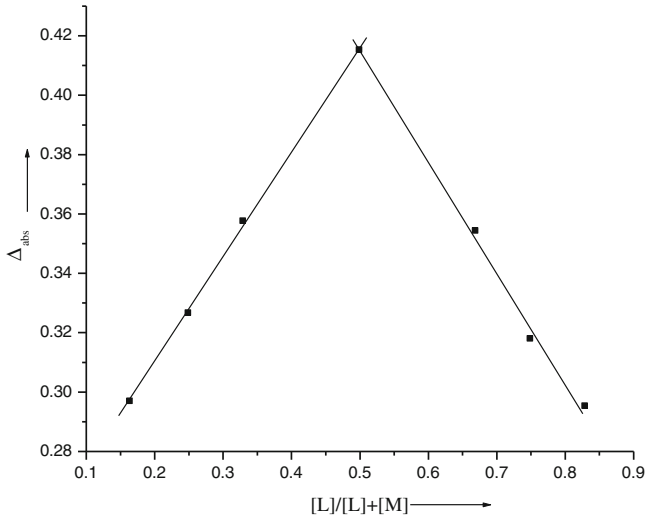

Figure 2. Job's plot: $[RuCl(Me_2SO)_3(H_2O)_2^+] = 1.0 \times 10^{-4}$ mol dm^{-3}, [diglycine] $= 1.0 \times 10^{-4}$ mol dm^{-3}, pH = 5.0.

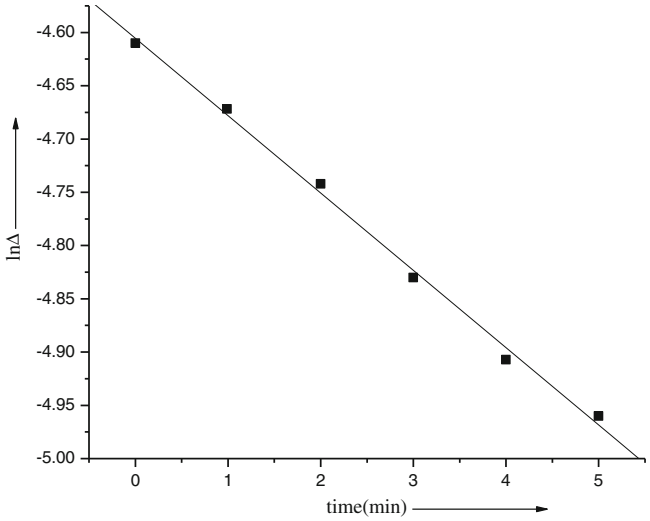

Figure 4. A typical plot of ln Δ versus time t. $[RuCl(Me_2SO)_3(H_2O)_2^+] = 1.0 \times 10^{-4}$ mol dm^{-3}, [diglycine] $= 2.0 \times 10^{-3}$ mol dm^{-3}, pH = 5.0, T = 50°C.

4. Results and discussion

The pK_a values of the ligands (gly gly), (gly ala) and (gly leu) are 3.21, 8.13,[36,37] 3.07, 8.12[38] and 3.18, 8.14,[39] respectively at 25°C. From the pK_a values of all the ligands we can say that at pH 5.0, all these three ligands remain in the zwitter ionic form.

The $\ln(A_\infty - A_t)$ *versus* time, (t) plot indicates that the reaction is not a single step process and a two step consecutive process may be assumed.

The rate constant for such a process can be evaluated by assuming the following scheme.

$$A \xrightarrow{k_1} B \xrightarrow{k_2} C$$

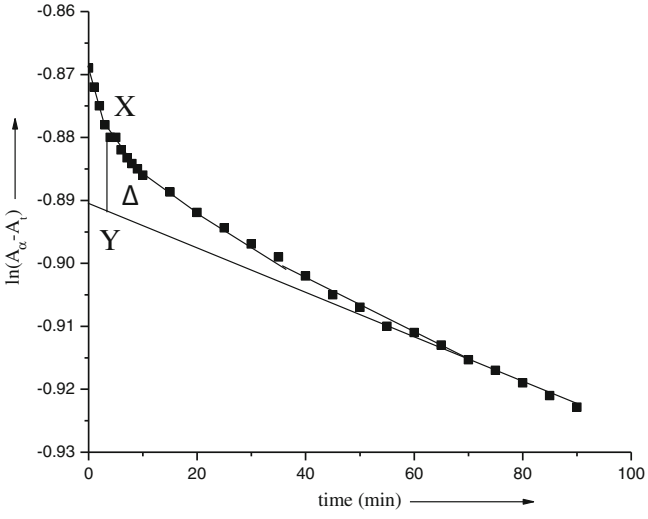

Figure 3. A typical plot of $\ln(A_\infty - A_t)$ versus time t. $[RuCl(Me_2SO)_3(H_2O)_2^+] = 1.0 \times 10^{-4}$ mol dm^{-3}, [diglycine] $= 2.0 \times 10^{-3}$ mol dm^{-3}, pH = 5.0, T = 50°C.

A is the substrate complex, B is the intermediate with ligand diglycine and C is the final product complex $[Ru(Me_2SO)_3(Cl)(L)]$.

4.1 *Calculation of k_1 value for A → B step*

The rate constant, $k_{1(obs)}$ for A → B step can be evaluated by the method of Weyh and Hamm using the usual consecutive rate law:

$$(A_\infty - A_t) = a_1 \exp\left(-k_{1(obs)}t\right) + a_2 \exp\left(-k_2 t\right)$$

or

$$(A_\infty - A_t) - a_2 \exp\left(-k_2 t\right) = a_1 \exp\left(-k_{1(obs)}t\right).$$

Table 1. 10^3 $k_{1(obs)}$ values for different ligand concentrations at different temperatures. [Complex-**1**] $= 1.0 \times 10^{-4}$ mol dm^{-3}, pH = 5.0.

Ligand	Temperature	10^3 [ligand] (mol dm^{-3})				
		1.00	2.00	3.00	4.00	5.00
gly gly	35	0.86	1.46	1.98	2.43	2.78
	40	1.14	1.96	2.58	3.13	3.70
	45	1.50	2.60	3.35	4.00	4.40
	50	1.92	3.40	4.18	4.81	5.25
gly ala	35	0.80	1.29	1.70	2.34	2.50
	40	1.18	1.86	2.78	3.03	3.50
	45	1.58	2.56	3.33	4.10	4.40
	50	1.90	3.10	4.40	5.18	5.58
gly leu	35	1.10	1.86	2.40	2.75	2.95
	40	1.35	2.12	2.66	3.10	3.25
	45	1.55	2.68	3.10	3.60	3.81
	50	2.00	2.95	3.45	3.93	4.10

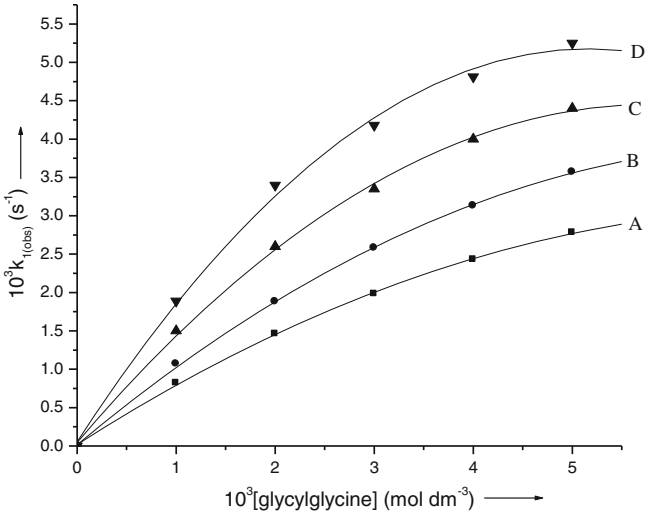

Figure 5. Plot of $k_{1(obs)}$ *versus* [diglycine] at different temperatures. A = 35, B = 40, C = 45, and D = 50°C.

Where a_1 and a_2 are constants dependent upon the rate constant and extinction coefficient. Values of $[(A_\infty - A_t) - a_2 \exp(-k_2 t)]$ are obtained from X–Y at different time (t) (figure 3). So ln Δ = constant – $k_{1(obs)}$ t. $k_{1(obs)}$ is derived from the slope of the ln Δ *versus* t (where t is small) (figure 4). A similar procedure is applied for each ligand concentration in the 1.00×10^{-3} mol dm^{-3} to 5.00×10^{-3} mol dm^{-3} range, at constant [(**1**)] (1.0×10^{-4} mol dm^{-3}) at pH = 5.0 and at different temperatures *viz*. 35, 40, 45 and 50°C, respectively. The $k_{1(obs)}$ values are listed in table 1.

The rate increases with increase in [ligand] and reaches a limiting value (figure 5), which is probable due to the completion of the outersphere association complex formation. Since the metal ion reacts with the immediate environment, further change in [ligand] beyond the saturation point will not affect the reaction rate and a gradual approach towards limiting rate is observed. At this stage, the interchange of the ligands from outer sphere to the inner sphere occurs,

Table 2. $10^3 k_{1(obs)}$ and K_{E1} values at different temperatures.

Ligand	Temperatures (°C)	10^3 k_1 (s^{-1})	K_{E1} (dm^{-3} mol^{-1} s^{-1})
Gly gly	35	5.89	170
	40	7.62	175
	45	8.77	206
	50	9.76	249
Gly ala	35	4.96	189
	40	6.66	213
	45	7.94	247
	50	8.76	285
Gly leu	35	2.35	131
	40	3.05	152
	45	3.85	175
	50	4.24	204

i.e., diglycine attacks the Ru(II) atom of the substrate complex and forms the intermediate.

Based on scheme 2 a rate expression can be derived for A → B step.

$$d[B]/dt = k_1 K_{E1} [B] [\text{ligand}] / (1 + K_{E1} [\text{ligand}]) \quad (1)$$

$$d[B]/dt = k_{1(obs)} [B]_T \quad (2)$$

T stands for total concentration of Ru(II). Thus it can be written,

$$k_{1(obs)} = k_1 K_{E1} [\text{ligand}] / (1 + K_{E1} [\text{ligand}]), \quad (3)$$

where k_1 is the rate constant for the formation of intermediate (B) from the substrate complex, *cis*-$[RuCl(Me_2SO)_3(H_2O)_2]^+$ (A). K_{E1} is the outersphere association equilibrium constant.

The equation can be written as

$$1/k_{1(obs)} = 1/k_1 + 1/k_1 K_{E1} [\text{ligand}]. \quad (4)$$

The plot of $1/k_{1(obs)}$ *versus* 1/ [ligand] should be linear (figure 6) with an intercept of $1/k_1$ and slope $1/k_1 K_{E1}$.

$$A + \text{ligand} \underset{}{\overset{K_{E1}}{\rightleftharpoons}} \text{A.ligand}$$

(outer sphere association complex)

$$\text{A.ligand} \xrightarrow{k_1} B$$

Scheme 2. Schematic representation for A→B.

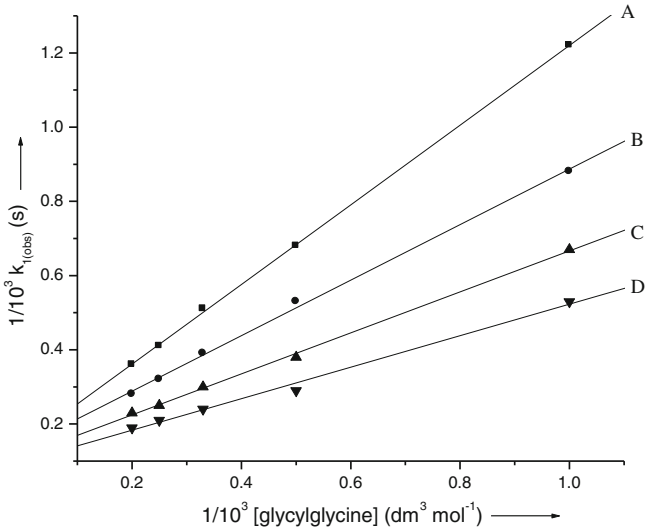

Figure 6. Plot of 1/ $k_{1(obs)}$ *versus* 1/[diglycine] at different temperatures, A = 35, B = 40, C = 45, and D = 50°C.

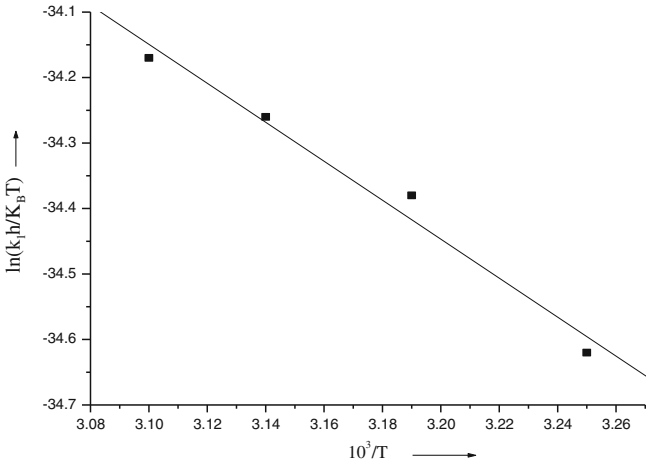

Figure 7. Eyring plot (ln k_1h/k_BT *versus* 1/T) for the step A → B (gly gly).

The k_1 and K_E values obtained from the intercept and from slope to intercept ratios are given in table 2.

4.2 *Calculation of k_2 for B → C step*

The B → C step is intramolecular ring closure and is independent of ligand concentration. At a particular temperature the slope of $\ln(A_\infty - A_t)$ *versus* time plot at different ligand concentrations was found to be constant in the region where the plot is linear (figure 3). For different temperatures the k_2 values are obtained directly from the limiting slope and the average 10^5k_2 values were (4.54, 6.35, 8.72 and 11.03 s^{-1}), (4.45, 6.23, 8.33, 10.24 s^{-1}) and (3.50, 5.89, 7.92, 10.16 unit) for glycyl glycine, glycyl alanine and glycyl-L-leucine at 35, 40, 45 and 50°C, respectively.

4.3 *Effect of temperature on the reaction rate*

Four different temperatures with varied ligand concentrations were chosen and the results are listed in table 3. The activation parameters for the step A → B and B → C are evaluated from the linear Eyring plots (figures 7 and 8).

The low $\Delta H^{\neq}$ values are in support of the ligand participation in the transition state for both steps. The positive energy required for the bond breaking process is partly compensated for by the negative energy obtained from bond formation in the transition state and, hence, a low value of $\Delta H^{\neq}$ is observed. The highly negative $\Delta S^{\neq}$ values, on the other hand, suggest a more compact transition state than the starting complexes and this is also in support of the assumption of a ligand participated transition state. $\Delta H_2^{\neq}$ is higher than $\Delta H_1^{\neq}$ which is quite expected for the second step which is slower than the first step.

5. Mechanism and conclusion

Our results indicate that the first step i.e., the attack by the incoming ligand (diglycine) proceed by an associative interchange (**Ia**) mechanism. This prediction is supported by the following facts. First, with an increase in ligand concentration saturation in rate is observed. This is possible only when an outer sphere association complex is formed. Secondly, the low enthalpy of

Table 3. Activation parameters for [complex-**1**] by diglycine in aqueous medium, pH = 5.0.

Ligand	$\Delta H_1^{\neq}$ (kJ mol^{-1})	$\Delta S_1^{\neq}$ (J K^{-1} mol^{-1})	$\Delta H_2^{\neq}$ (k J mol^{-1})	$\Delta S_2^{\neq}$ (J K^{-1} mol^{-1})	ref.
Azide	20.1 ± 3.49	−162 ± 11	35.5 ± 4.2	−105 ± 13	40
gly gly	24.7 ± 2.6	−207 ± 8	46.8 ± 0.8	−176 ± 2	29
gly ala	28.1 ± 3.9	−198 ± 12	52.6 ± 2.45	−154 ± 7	This work
gly leu	30.3 ± 1.0	−191 ± 5	56.0 ± 3.95	−148 ± 12	This work

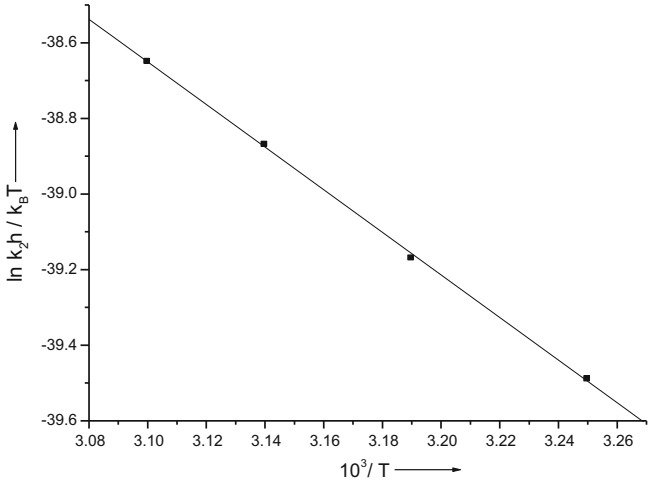

Figure 8. Eyring plot (ln k_2h/k_BT *versus* 1/ T) for the step B → C (gly gly).

activation and large negative value of entropy of activation strongly suggest the ligand participation in the transition state. In the first step, a rapid equilibrium is established, resulting in outer sphere complex (ion pair) between complex-**1** and ligand diglycine. Then the ion-pair is transformed to mono bonded complex which is the rate limiting first step (k_1). The second step is the intramolecular ring closure which is independent of the incoming ligand concentration. This is supported by the values of rate constant (k_2); for this step k_2 values were found to be independent of ligand concentration. From the temperature dependence of the K_{E1}, the thermodynamic parameters are calculated: $\Delta H_1^0 = 21.0 \pm 5.3$, 20.4 ± 1.8, 21.2 ± 1.6 kJ mol^{-1}and $\Delta S_1^0 = 111 \pm 14$, 135 ± 6, 137 ± 5 J K^{-1} mol^{-1}.

From IR spectra, it was seen that –COO^- is involved in complexation through O^- centre and amide –NH centre. As the electron density on O^- is greater than that of amide N centre, O^- follows k_1 path and N follows k_2 path. The final product is a five membered chelate involving the carboxylate (O^-) and amide (N) centres of the dipeptides.

From a comparison of the dipeptides used, it can be concluded that the variation in size and bulkiness of the coordinating dipeptides indicates their functional properties as nucleophiles. The sensitivity of the reaction rate towards the donor properties of the entering

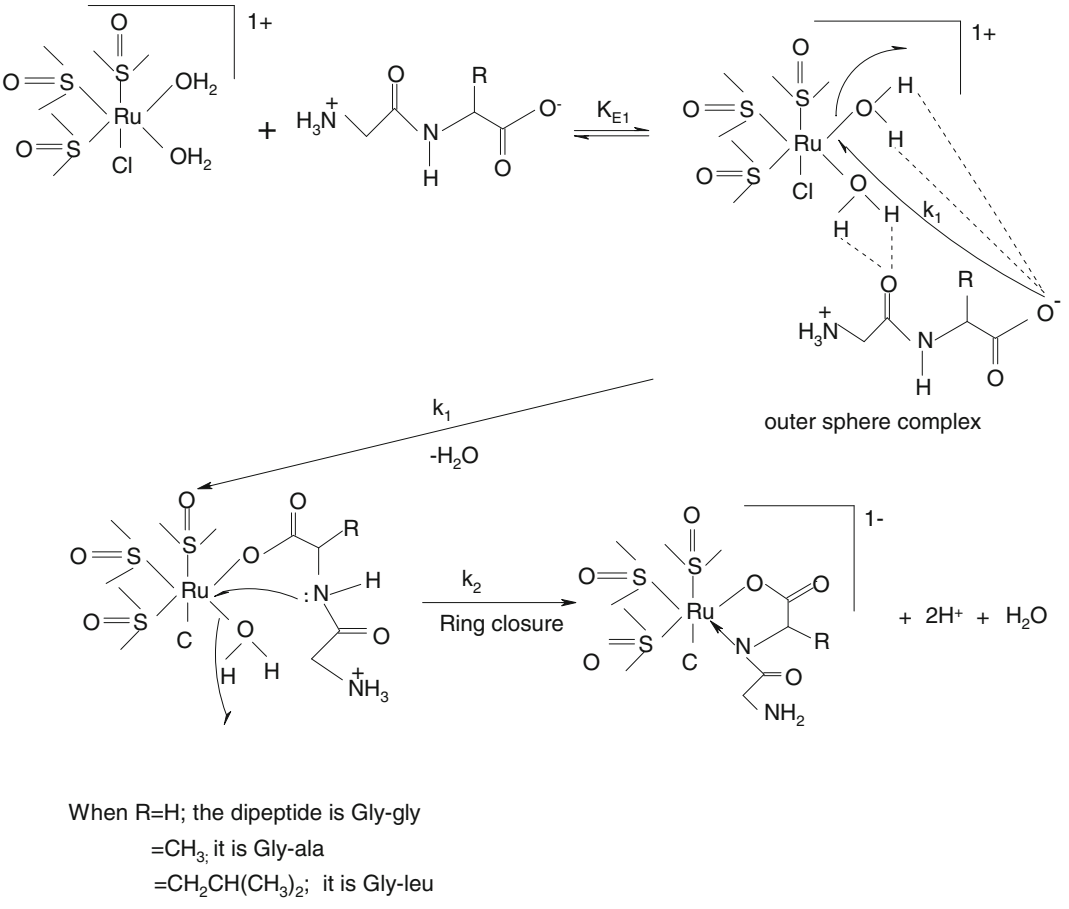

Figure 9. Plausible mechanism for the substitution of aqua ligands from *cis*-$[RuCl(Me_2SO)_3(H_2O)_2]^+$ by dipeptides.

ligands is in the line with that expected for an associative mode of activation. The differences in reactivity of the selected dipeptides is obvious and their reactivity follows the order Gly-L-leu < Gly-L-ala < Gly-gly. In addition, steric effects are very important as well. For the three dipeptides with increasing steric effects reactivity decreases which reflect in their rate constants values. So from IR data, conductance measurement and Job's plot a plausible mechanism may be shown in the following scheme (figure 9).

Acknowledgements

The authors acknowledge the assistance received from the University of Burdwan. One of the authors (AM) is indebted to the University Grants Commission (UGC), New Delhi, India for providing a fellowship to him. Authors are also indebted to Dr. P Chattopadhyay for his help in preparing the starting material.

References

1. Rosenberg B, Vancamp L and Krigas T 1965 *Nature (London)* **205** 698
2. Esposito B P and Najjar R 2002 *Coord. Chem. Rev.* **232** 127
3. Banerjee D, Kadam T A and Sigal H 1981 *Inorg. Chem.* **20** 2586
4. Umapathy P 1989 *Coord. Chem. Rev.* **95** 129
5. Clarke M J 1980 in: Martell A E (ed.), *Inorg. Chem. in Biol. and Med., (ACS Symp. Ser. 140) Am. Chem. Soc., Wasington DC*, 157 and references cited therein
6. Pruchnik P F, Bien M, Lakowicz T and Tadeusz 1996 *Met. Based Drugs* **4** 185
7. Clarke M J 1980 *Met. Ions Biol. Syst.* **11** 231
8. Yasbin R E, Matthews C R and Clarke M J 1980 *Chem. Biol. Interact.* **31** 355
9. Reedijk J 1987 *Pure & Appl. Chem.* **59** 181
10. Zhao M and Clarke M J 1999 *J. Biol. Chem.* **4** 325
11. Galardon E, Maux P Lc, Bondon A and Simonncaux G 1999 *Tetrahedron: Asymmetry* **10** 4203
12. Frasca D R and Clarke M J 1999 *J. Am. Chem. Soc.* **121** 8523
13. Povsc V G and Olabe J A 1998 *Transition Met. Chem.* **23** 657
14. Izumi H K and Smith W L 2000 *Abstracts of papers of the Am. Chem. Soc.* **219** 727
15. Wang Z M and Ji L N 2002 *Prog. Chem.* **14** 296
16. Roncaroli F, Ruggiero M E, Franco D W, Estiu G L and Olabe J A 2002 *Inorg. Chem.* **41** 5760
17. Harthmann M, Lipponer K-G and Keppler B K 1998 *Inorg. Chim. Acta* **267** 137
18. Turel I, Pecanac M, Golobic A, Allessio E and Serli B 2002 *Eur. J. Inorg. Chem.* 1928
19. Leudtke N W, Hwang J S, Glazer E C, Gut D, Kol M and Tor Y 2002 *Chembiochem* **3** 766
20. Shailendra Bharti N, Garza M T G, Guzvega D E, Garza J C, Saliem K, Naqv M and Zam A 2001 *Bioorg. Med. Chem. Lett.* **11** 2675
21. Allessio E, Iengo E, Serli B, Mestroni G and Sava G 2001 *J. Inorg. Biochem.* **86** 21
22. Ang W H and Dyson P J 2006 *Eur. J. Inorg. Chem.* **20** 4003
23. Clarke M J 2003 *Coord. Chem. Rev.* **236** 209
24. Komeda S, Moulaei T, Woods K K, Chikuma M, Farrell N P and Williams L D 2006 *J. Am. Chem. Soc.* **128** 16092
25. Hannon M J 2007 *Chem. Soc. Rev.* **36** 280
26. Pitteri C and Cini R 1998 *J. Chem. Soc., Dalton Trans.* 2679
27. Sulu M, Kucukbay H, Durmaz R and Gunal S 2000 *Microbiologica* **23** 73
28. Zhen Q X, Ye B H, Liu J G, Zhang Q L, Ji L N and Wang L 2000 *Inorg. Chim. Acta* **303** 141
29. Mandal A, Bera B K, Mallick S, Mondal S, Karmakar P and Ghosh A K 2011 *Int. J. Life Sci. Pharma Res.* **1** 110
30. Evans I P, Spencer A and Wilkinson G 1973 *J. Am. Chem. Soc., Dalton Trans.* 204
31. Enzo Alessio, Giovanni Mestroni, Giorgio Nardin, Wahib M. Attia, Mario Calligaris, Gianni Sava and Sonia Zoret 1988 *Inorg. Chem.* **27** 4099
32. Barnes J R and Goodfellow R J 1976 *J. Chem. Res., Miniprint* 4301
33. Nath M, Pokharia S, Eng G, Song X and Kumar A 2004 *Synthesis and reactivity in inorganic and metal-organic chemistry* **34** 1689
34. Mercer E E, McAllister W A and Durig J R 1966 *Inorg. Chem.* **5** 1881
35. Weyh J A and Hamm R E 1969 *Inorg. Chem.* **8** 2298
36. Kim M K and Martell A E 1984 *Biochemistry* **3** 1169
37. Sigel H, Griesser R and Prijs B 1972 *Z Naturforsch (B)* **27** 353
38. Martell A E and Smith R M 1974 *Critical Stability Constants*, vol. 1 (New York, NY, USA: Plenum Press) 297
39. Martell A E and Smith R M 1974 *Critical stability constants*, vol. 1 (New York, NY, USA: Plenum Press) 299
40. Mandal A, Bera B K, Mallick S, Mondal S, Karmkar P and Ghosh A K 2010 *Inorg. Chem. Indian J.* **5**(4) 176